Azimuthal seismic inversion for fracture weaknesses based on facies constraint

Huaizhen Chen*, Jian Han†,and Kristopher A. Innanen

ABSTRACT

A two-step inversion method of employing azimuthal seismic data to estimate fracture weaknesses constrained by fracture facies constraint is proposed. Firstly, based on the PP-wave reflection coefficient and azimuthal elastic impedance (EI) derived in terms of elastic properties, density and fracture weaknesses, we use a Bayesian Markov chain Monte Carlo (MCMC) algorithm to estimate EI of different incidence angles and azimuths, and predict fracture facies using the estimated EI. Secondly, we use the fracture facies to construct a more accurate initial model of unknown parameters(M, μ, ρ, δ_N and δ_T) and use the estimated EI of different incidence angles and azimuths as the input to estimate unknown parameters. Employing noisy seismic data of signal-to-noise ratios (S/N), we verify the robustness of the proposed inversion method.

INTRODUCTION

Subsurface natural fractures are important channels for oil and gas migration and storage. Using seismic data to implement predict the characteristics of underground fractures with high accuracy is of great significance.

Rock physics effective model plays an important role in relating fracture properties (e.g. fracture density, aspect ratio, fracture fillings) to elastic properties (e.g. stiffness coefficients, velocity) of fractured rock. Schoenberg and Sayers (1995) proposed the linear-slip model, in which two dimensionless parameters, the normal and tangential fracture weaknesses (δ_N and δ_T) are presented to measure how fractures affect the displacement component perpendicular and parallel to the fracture plane. Fracture weaknesses become two important indicators, which are used to characterize underground fractures, and methods of inversion of azimuthal seismic data for estimating fracture weaknesses has been presented.

Based on the linear-slip model, Chen et al. (2014, 2018) proposed azimuthal elastic impedance (EI) expressed in terms of δ_N and δ_T and implement the simultaneous inversion for elastic properties of isotropic background and fracture weaknesses. Estimation of elastic parameters and fracture weaknesses based on azimuthal EI has many advantages, such as the input data is azimuthally incidence-angle-stacked seismic data, which is of a relatively high signal to noise ratio (SNR), and the inversion of stacked seismic data for estimating EI is more stable than the inversion of amplitude-versus-offset (AVO) data for estimating elastic parameters and fracture weaknesses, which is ill conditioned. However, due to the noise existing in seismic observation data and the error accumulation of two-step inversion (inversion for EI in the first step, and using EI to estimate elastic parameters and

*School of Ocean and Earth Science, Tongji University, Shanghai, China; and CREWES Project, University of Calgary, Calgary, Alberta, Canada. Email: huaizhen.chen@ucalgary.ca

†School of Ocean and Earth Science, Tongji University, Shanghai, China

fracture weaknesses in the second step.) is relatively larger than that of single-step inversion (inversion of azimuthal AVO data to estimate parameters and fracture weaknesses), the first-step inversion should be more robust and produce azimuthal EI results of relatively high, and the second-step inversion should be more stable and provide more reliable estimate of elastic parameters and fracture weaknesses. In the present study, we aim to use a more reliable and accurate initial model to constrain the two-step inversion, and additional information, i.e. fracture facies, is considered to construct the initial models.

Currently, lithology facies, are used to constrain seismic inversion for elastic parameters (e.g. P- and S-wave velocities) and reservoir parameters (e.g. porosity, shale content, water saturation). Grana (2018) implemented the simultaneous estimation of lithofacies, porosity, clay volume, and water saturation using a nonparametric distribution of Bayesian Gaussian mixture model. Similar to the role of lithology facies in seismic inversion for reservoir characterization, we extract fracture facies from seismic data and involve the fracture facies as a constraint in the estimation of elastic parameters of isotropic background and fracture weaknesses.

We propose a two-step inversion method of employing azimuthal seismic data to estimate elastic parameters of isotropic background and fracture weaknesses. Firstly, we use azimuthally incidence-angle-stacked seismic data as the input and employ the Bayesian Markov chain Monte Carlo (MCMC) to obtain azimuthal EI and fracture facies; and secondly, following the Bayesian framework again, we implement the estimation of elastic parameters and fracture weaknesses constrained by fracture facies. We use noisy synthetic seismic data to verify the robustness of the proposed inversion method.

THEORY AND METHOD

In this section, we present how to obtain fracture facies information during the inversion of azimuthally partially incidence-angle-stacked seismic data for EI, and how to implement the inversion of azimuthal EI for fracture weaknesses under the constraint of fracture facies.

Estimation of azimuthal elastic impedance and facies

Stiffness matrix of a rock that contains a set of vertical fractures is given by (Schoenberg and Sayers, 1995)

$$\mathbf{C} = \begin{bmatrix} M(1-\delta_N) & (M-2\mu)(1-\delta_N) & (M-2\mu)(1-\delta_N) & 0 & 0 & 0 \\ (M-2\mu)(1-\delta_N) & M\left(1-\chi^2\delta_N\right) & (M-2\mu)(1-\chi\delta_N) & 0 & 0 & 0 \\ (M-2\mu)(1-\delta_N) & (M-2\mu)(1-\chi\delta_N) & M\left(1-\chi^2\delta_N\right) & 0 & 0 & 0 \\ 0 & 0 & 0 & \mu & 0 & 0 \\ 0 & 0 & 0 & 0 & \mu(1-\delta_T) & 0 \\ 0 & 0 & 0 & 0 & 0 & \mu(1-\delta_T) \end{bmatrix}, \tag{1}$$

where M and μ are P- and S-wave moduli of the isotropic background rock, $\chi = (M-2\mu)/M$, and δ_N and δ_T are the normal and tangential fracture weaknesses, respectively.

We use a relationship between reflection coefficient and perturbation in stiffness parameters to derive a linearized PP-wave reflection coefficient R_{PP} as a function of reflectivities

of P- and S-wave moduli ($\frac{\Delta M}{2M}$, $\frac{\Delta \mu}{2\mu}$), density ($\frac{\Delta \rho}{2\rho}$) and changes in fracture weaknesses ($\Delta\delta_N$, $\Delta\delta_T$) across the reflection interface

$$\begin{aligned} R_{PP}(\theta,\phi) =& a_M(\theta)\frac{\Delta M}{M} + a_\mu(\theta)\frac{\Delta \mu}{\mu} + a_\rho(\theta)\frac{\Delta \rho}{\rho} \\ &+ a_N(\theta,\phi)\Delta\delta_N + a_T(\theta,\phi)\Delta\delta_T, \end{aligned} \tag{2}$$

where θ is angle of incidence, ϕ is angle of azimuth,

$$\begin{aligned} a_M(\theta) &= \frac{1}{4}\sec^2\theta, \\ a_\mu(\theta) &= -2\,g\sin^2\theta, \\ a_\rho(\theta) &= \frac{\cos 2\theta}{4\cos^2\theta}, \\ a_N(\theta,\phi) &= -\frac{1}{4\cos^2\theta}\left[2g\left(\sin^2\theta\sin^2\phi + \cos^2\theta\right) - 1\right]^2, \\ a_T(\theta,\phi) &= -g\sin^2\theta\cos^2\phi\left(\tan^2\theta\sin^2\phi - 1\right). \end{aligned} \tag{3}$$

From the derived PP-wave reflection coefficient, azimuthal EI emerges as

$$EI(\theta,\phi) = M^{2a_M(\theta)}\,\mu^{2a_\mu(\theta)}\,\rho^{2a_\rho(\theta)}\exp\left[a_N(\theta,\phi)\,\delta_N + a_T(\theta,\phi)\,\delta_T\right]. \tag{4}$$

We write the nonlinear relationship between the vector of EI (i.e. $\mathbf{m}$) and the vector of seismic data (i.e. $\mathbf{d}$) as

$$\mathbf{d} = \mathbf{G}(\mathbf{m}), \tag{5}$$

where $\mathbf{G}$ is the nonlinear forward modeling operator.

Based on Bayesian theorem, we make probabilistic estimates of EI and fracture facies from seismic data of incidence angle θ and azimuth ϕ. Considering the fracture facies $\mathbf{f}$ as another unknown parameter vector and introducing the distribution of fracture facies $P(\mathbf{f})$ into the posterior probability of $\mathbf{m}$ given $\mathbf{d}$, we express the posterior probability distribution function, i.e. $P(\mathbf{m},\mathbf{f}|\mathbf{d})$, as

$$P(\mathbf{m},\mathbf{f}|\mathbf{d}) \propto P(\mathbf{d}|\mathbf{m},\mathbf{f})\,P(\mathbf{m},\mathbf{f}) \propto P(\mathbf{d}|\mathbf{m})\,P(\mathbf{m}|\mathbf{f})\,P(\mathbf{f}), \tag{6}$$

where $P(\mathbf{d}|\mathbf{m},\mathbf{f})$ is the likelihood function, $P(\mathbf{m},\mathbf{f})$ is the prior distribution that contains two components: 1) the likelihood function that expresses the probability of $\mathbf{m}$ given $\mathbf{f}$, i.e. $P(\mathbf{m}|\mathbf{f})$; and 2) the distribution of fracture facies, $P(\mathbf{f})$. We emphasize that we assume the probability of $\mathbf{d}$ given $\mathbf{m}$ and $\mathbf{f}$ mainly depends on $\mathbf{m}$, therefore, we approximately write the likelihood $P(\mathbf{d}|\mathbf{m},\mathbf{f})$ as $P(\mathbf{d}|\mathbf{m})$.

To solve the nonlinear inversion problem, we employ the Markov chain Monte Carlo algorithm to generate a few of acceptable results of EI and facies. Assuming two likelihood

functions $P(\mathbf{d}|\mathbf{m})$ and $P(\mathbf{m}|\mathbf{f})$ are Gaussian distribution and fix the facies, we first estimate EI using partially incidence-angle-stacked seismic data of different azimuthal angles. The acceptance ratio used to determine whether to keep the candidate of $\mathbf{m}$ is given by

$$r = \min\left\{1, \exp\left(-\left[E\left(\mathbf{m}^*\right) - E\left(\mathbf{m}\right)\right]\right)\right\}, \tag{7}$$

where $\mathbf{m}^*$ is the candidate, and

$$E(\mathbf{m}) = [\mathbf{d} - \mathbf{G}(\mathbf{m})]^T [\mathbf{d} - \mathbf{G}(\mathbf{m})] + \left(\frac{1}{2}\Delta \ln \mathbf{m} - s\Delta\mathbf{f}\right)^T \left(\frac{1}{2}\Delta \ln \mathbf{m} - s\Delta\mathbf{f}\right), \tag{8}$$

where s is a scale factor, $\ln \mathbf{m}$ is the logarithmic value of $\mathbf{m}$, and Δ is the differential operator.

In Figure 1, we show EI curve of a layered model, corresponding fracture facies, and comparison between reflectivity computed using EI and fracture facies. We observe that

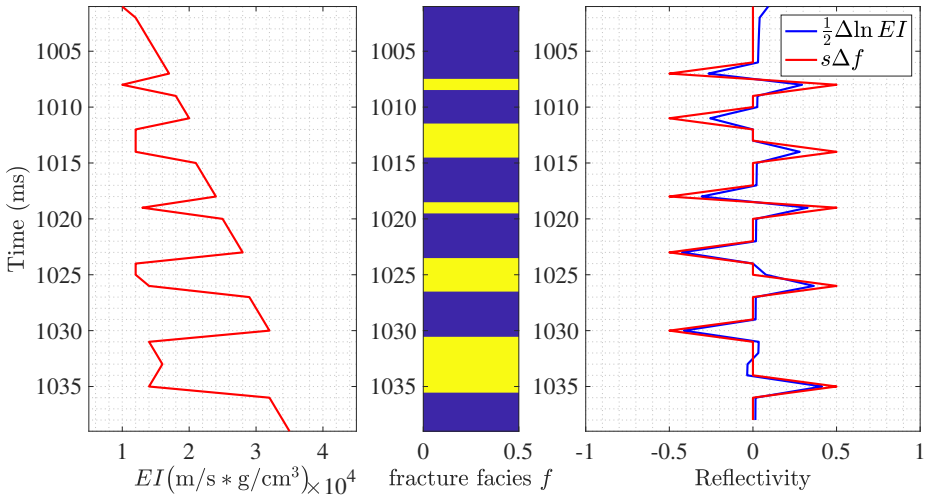

FIG. 1. A layered model. The scale factor s is 0.5.

the locations of quasi-reflectivity calculated using the scaled fracture facies match that of the true-reflectivity calculated using the logarithmic EI, and at some locations the value of quasi-reflectivity is also close to that of the true-reflectivity. It verifies that we may use the fracture facies to constrain the inversion for EI, as shown in equation 8.

We proceed to the estimation of fracture facies using the estimated EI of different incidence angles and azimuths. Following the Bayesian framework again, we present the posterior probability of $s\Delta\mathbf{f}$ (denoted by $\mathbf{Df}$) given $\frac{1}{2}\Delta \ln \mathbf{m}$ (denoted by $\mathbf{Dm}$) as

$$P(\mathbf{Df}|\mathbf{Dm}) \propto P(\mathbf{Dm}|\mathbf{Df})\, P(\mathbf{Df}), \tag{9}$$

and we implement a most likely estimate of fracture facies. Under the assumption that the likelihood function $P(\mathbf{Df}|\mathbf{Dm})$ is Gaussian and the prior distribution $P(\mathbf{Df})$ is Cauchy, which may create a sparse spike series of fracture facies, we write the objective function as

$$J(\mathbf{Df}) = \frac{(\mathbf{Dm} - \mathbf{Df})^T (\mathbf{Dm} - \mathbf{Df})}{2\sigma_{\mathbf{n}}^2} + \sum_{i=1}^{N-1} \ln\left[1 + \frac{(Df_i)^2}{\sigma_{\mathbf{Df}}^2}\right], \tag{10}$$

where $\sigma_{\mathbf{n}}^2$ is variance of the difference between $\mathbf{Dm}$ and $\mathbf{Df}$, $\sigma_{\mathbf{Df}}^2$ is variance of the differential of fracture facies, and N is the number of underground layers.

Taking the derivative of $J(\mathbf{Df})$

$$\frac{\partial J(\mathbf{Df})}{\partial \mathbf{Df}} = 0, \tag{11}$$

results in

$$\left(\mathbf{I} + \frac{2\sigma_{\mathbf{n}}^2}{\sigma_{\mathbf{Df}}^2}\mathbf{L}\right)\mathbf{Df} = \mathbf{Dm}, \tag{12}$$

where $\mathbf{I}$ is an identity matrix, and

$$\mathbf{L}_{ii} = \left[1 + \frac{(Df_i)^2}{\sigma_{\mathbf{Df}}^2}\right]^{-1}. \tag{13}$$

Given an initial model of fracture facies constructed using Formation Micro-Imager (FMI) logging data, the inverse problem is solved iteratively to obtain results of $\mathbf{Df}$. Using the inversion results of $\mathbf{Df}$, we may obtain the estimated fracture facies $\mathbf{f}$.

Inversion for fracture weaknesses constrained by fracture facies

Using the estimated EI of different incidence angles and azimuths, we proceed to the inversion for elastic properties (M, μ), bulk density (ρ) and fracture weaknesses (δ_N and δ_T). Taking a logarithm of EI yields

$$L_{EI}(\theta,\phi) = 2a_M(\theta)L_M + 2a_\mu(\theta)L_\mu + 2a_\rho(\theta)L_\rho + a_N(\theta,\phi)\,\delta_N + a_T(\theta,\phi)\,\delta_T, \tag{14}$$

where L_{EI}, L_M, L_μ and L_ρ represent the logarithmic EI, M, μ and ρ, respectively.

Considering N layers, two incidence angles and two azimuths, equation 14 becomes

$$\mathbf{B} = \mathbf{Ax}, \tag{15}$$

where

$$\mathbf{B} = \begin{bmatrix} \mathbf{L_{EI}}(\theta_1,\phi_1) \\ \mathbf{L_{EI}}(\theta_2,\phi_1) \\ \mathbf{L_{EI}}(\theta_1,\phi_2) \\ \mathbf{L_{EI}}(\theta_2,\phi_2) \end{bmatrix}, \tag{16}$$

$$\mathbf{A} = \begin{bmatrix} \mathbf{p}_M(\theta_1) & \mathbf{p}_\mu(\theta_1) & \mathbf{p}_\rho(\theta_1) & \mathbf{p}_N(\theta_1,\phi_1) & \mathbf{p}_T(\theta_1,\phi_1) \\ \mathbf{p}_M(\theta_2) & \mathbf{p}_\mu(\theta_2) & \mathbf{p}_\rho(\theta_2) & \mathbf{p}_N(\theta_2,\phi_1) & \mathbf{p}_T(\theta_2,\phi_1) \\ \mathbf{p}_M(\theta_1) & \mathbf{p}_\mu(\theta_1) & \mathbf{p}_\rho(\theta_1) & \mathbf{p}_N(\theta_1,\phi_2) & \mathbf{p}_T(\theta_1,\phi_2) \\ \mathbf{p}_M(\theta_2) & \mathbf{p}_\mu(\theta_2) & \mathbf{p}_\rho(\theta_2) & \mathbf{p}_N(\theta_2,\phi_2) & \mathbf{p}_T(\theta_2,\phi_2) \end{bmatrix}, \tag{17}$$

$$\mathbf{x} = \begin{bmatrix} \mathbf{L_M} \\ \mathbf{L_u} \\ \mathbf{L_d} \\ \mathbf{L_N} \\ \mathbf{L_T} \end{bmatrix}, \tag{18}$$

where

$$\mathbf{L_{EI}}(\theta,\phi) = \begin{bmatrix} L_{EI}^{(1)}(\theta,\phi) \\ \vdots \\ L_{EI}^{(N)}(\theta,\phi) \end{bmatrix}, \ \mathbf{L_M} = \begin{bmatrix} L_M^{(1)} \\ \vdots \\ L_M^{(N)} \end{bmatrix}, \ \mathbf{L_u} = \begin{bmatrix} L_\mu^{(1)} \\ \vdots \\ L_\mu^{(N)} \end{bmatrix},$$

$$\mathbf{L_d} = \begin{bmatrix} L_\rho^{(1)} \\ \vdots \\ L_\rho^{(N)} \end{bmatrix}, \ \mathbf{L_N} = \begin{bmatrix} \delta_N^{(1)} \\ \vdots \\ \delta_N^{(N)} \end{bmatrix}, \ \mathbf{L_T} = \begin{bmatrix} \delta_T^{(1)} \\ \vdots \\ \delta_T^{(N)} \end{bmatrix},$$

$$\mathbf{p}_M(\theta) = \begin{bmatrix} 2a_M^{(1)}(\theta) & \\ & 2a_M^{(2)}(\theta) \end{bmatrix}, \ \mathbf{p}_\mu(\theta) = \begin{bmatrix} 2a_\mu^{(1)}(\theta) & \\ & 2a_\mu^{(2)}(\theta) \end{bmatrix},$$

$$\mathbf{p}_\rho(\theta) = \begin{bmatrix} 2a_\rho^{(1)}(\theta) & \\ & 2a_\rho^{(2)}(\theta) \end{bmatrix}, \ \mathbf{p}_N(\theta,\phi) = \begin{bmatrix} a_N^{(1)}(\theta,\phi) & \\ & a_N^{(2)}(\theta,\phi) \end{bmatrix},$$

$$\mathbf{p}_T(\theta,\phi) = \begin{bmatrix} a_T^{(1)}(\theta,\phi) & \\ & a_T^{(2)}(\theta,\phi) \end{bmatrix}, \tag{19}$$

where the superscript indicate the layer number.

In the forward modeling to produce the vector of L_{EI}, we assume difference between the modeled result and the input data follow Gaussian distribution. Considering a univariate Cauchy prior distribution, we express the posterior probability of $\mathbf{x}$ given $\mathbf{B}$ in the case of N layers as

$$\begin{aligned} P(\mathbf{x}|\mathbf{B}) &\propto P(\mathbf{B}|\mathbf{X})\, P(\mathbf{x}) \\ &\propto \exp\left[-\frac{(\mathbf{B}-\mathbf{A}\mathbf{x})^T (\mathbf{B}-\mathbf{A}\mathbf{x})}{2\sigma_{\mathbf{e}}^2} - \sum_{i=1}^{5N} \ln\left(1 + \frac{(x_i - \mathbf{x}_a)^T (x_i - \mathbf{x}_a)}{\sigma_{\mathbf{x}}^2} \right) \right], \end{aligned} \tag{20}$$

where $\sigma_{\mathbf{e}}^2$ is the variance of difference between the modeled and input data of $\mathbf{B}$, $\mathbf{x}_a$ is the average of $\mathbf{x}$, and $\sigma_{\mathbf{x}}^2$ is the variance of $\mathbf{x}$, respectively.

The objective function used to make a best estimate of unknown parameter vector $\mathbf{x}$ is proposed based on the maximum of posterior probability. Using model constraints, we

write the final expression of the objective function as

$$\begin{aligned} J(\mathbf{x}) =& \frac{(\mathbf{B}-\mathbf{A}\mathbf{x})^T(\mathbf{B}-\mathbf{A}\mathbf{x})}{2\sigma_{\mathbf{e}}^2} + \sum_{i=1}^{5N} \ln\left[1+\frac{(x_i-\mathbf{x}_a)^T(x_i-\mathbf{x}_a)}{\sigma_{\mathbf{x}}^2}\right] \\ &+ W_M(\mathbf{L_M}-\mathbf{L_{M0}})^T(\mathbf{L_M}-\mathbf{L_{M0}}) + W_\mu(\mathbf{L_u}-\mathbf{L_{u0}})^T(\mathbf{L_u}-\mathbf{L_{u0}}) \\ &+ W_\rho(\mathbf{L_d}-\mathbf{L_{d0}})^T(\mathbf{L_d}-\mathbf{L_{d0}}) + W_N(\mathbf{L_N}-\mathbf{L_{N0}})^T(\mathbf{L_N}-\mathbf{L_{N0}}) \\ &+ W_T(\mathbf{L_T}-\mathbf{L_{T0}})^T(\mathbf{L_T}-\mathbf{L_{T0}}), \end{aligned} \tag{21}$$

where W_M, W_μ, W_ρ, W_N and W_T are weight factors of model constraints, $\mathbf{L_{M0}}$, $\mathbf{L_{u0}}$, $\mathbf{L_{d0}}$, $\mathbf{L_{N0}}$ and $\mathbf{L_{T0}}$ are model constrains of P- and S-wave moduli, density and fracture weaknesses, respectively.

A more reliable initial model leads to a better inversion result of unknown parameter vector. Using the fractured facies obtained in the previous step of inversion for EI, we construct new initial models of $\mathbf{L_M}$, $\mathbf{L_u}$, $\mathbf{L_d}$, $\mathbf{L_N}$ and $\mathbf{L_T}$ as

$$\begin{aligned} \mathbf{L_{M0}} &= \mathbf{L_M^{low}} + s_M\,\mathbf{f}, \\ \mathbf{L_{u0}} &= \mathbf{L_u^{low}} + s_\mu\,\mathbf{f}, \\ \mathbf{L_{d0}} &= \mathbf{L_d^{low}} + s_\rho\,\mathbf{f}, \\ \mathbf{L_{N0}} &= \mathbf{L_N^{low}} + s_N\,\mathbf{f}, \\ \mathbf{L_{T0}} &= \mathbf{L_T^{low}} + s_T\,\mathbf{f}, \end{aligned} \tag{22}$$

where $\mathbf{L_M^{low}}$, $\mathbf{L_u^{low}}$, $\mathbf{L_d^{low}}$, $\mathbf{L_N^{low}}$ and $\mathbf{L_T^{low}}$ represent low frequency components of P- and S-wave moduli, density and fracture weaknesses, and s_M, s_μ, s_ρ, s_N and s_T represent scale factors that determine how fracture facies contributes to initial models.

Taking the derivative of $J(\mathbf{x})$

$$\frac{\partial J(\mathbf{x})}{\partial \mathbf{x}} = 0 = \mathcal{H} - \mathcal{G}\,\mathbf{x}, \tag{23}$$

results in the solution of $\mathbf{x}$

$$\mathbf{x}_{i+1} = \mathbf{x}_i + \left(\mathcal{G}^T\mathcal{G}\right)^{-1}\mathcal{G}^T(\mathcal{H} - \mathcal{G}\,\mathbf{x}_i), \tag{24}$$

where $\mathbf{x}_i$ is an initial model of unknown parameter vector. Using the iterative algorithm as shown in equation 24, we obtain the inversion results of M, μ, ρ, δ_N and δ_T.

NUMERICAL EXAMPLES: SYNTHETIC

In this section, we use synthetic data generated for a well log model to verify the robustness of the proposed inversion algorithm. Curves of P- and S-wave moduli and density are shown in Figure 2. Fracture weaknesses δ_N and δ_T, and the reference fracture facies constructed based on the tangential fracture weakness δ_T (i.e. interpreting the area where $\delta_T \geq 0.11$ as fractured reservoir and setting the corresponding f to 1), are shown in Figure 3.

We add Gaussian random noise to synthetic data generated based on the convolution model to produce noisy seismic data of signal-to-noise ratio (S/N) of 4 and 1. Using the noisy synthetic seismic data as the input, we implement the inversion for EI of different incidence and azimuthal angles. In Figures 4 and 5, we show comparisons between the inversion results and true values of EI.

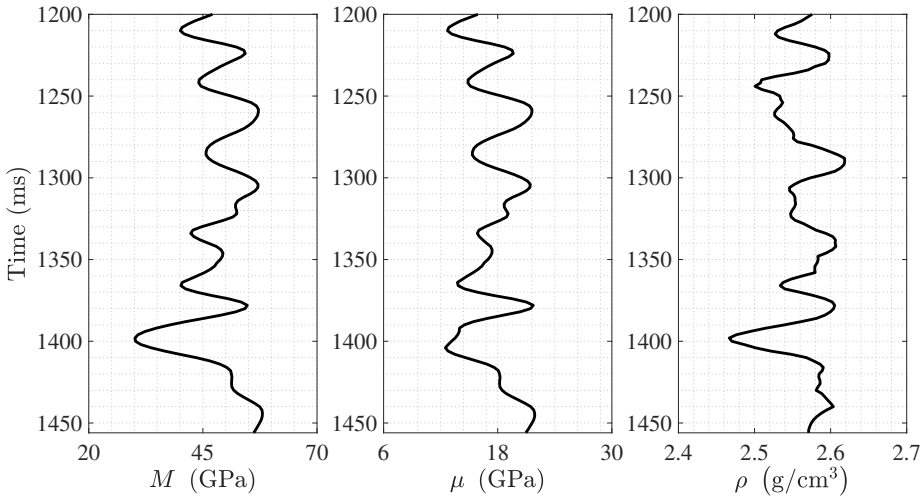

FIG. 2. A well log model: Curves of P- and S-wave moduli and density

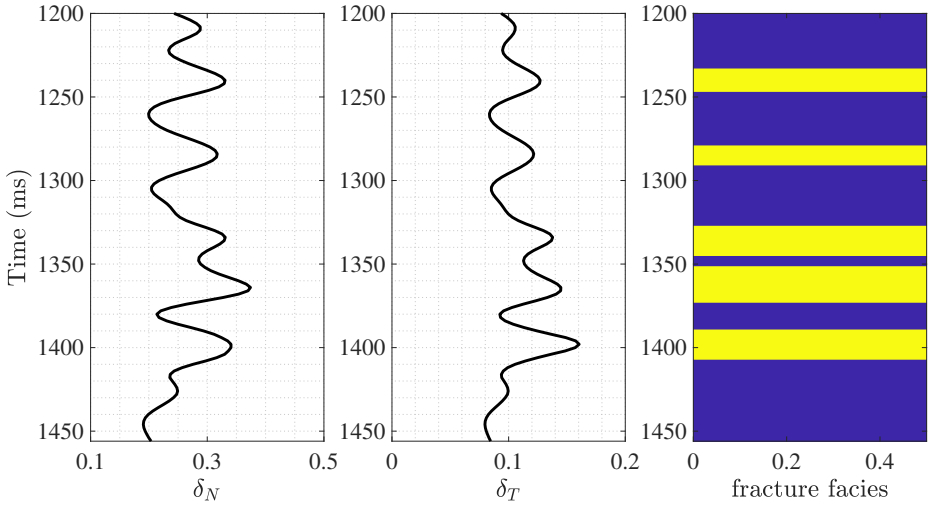

FIG. 3. A well log model: Curves of fracture weaknesses and the constructed fracture facies

Using the inversion results of EI, we next implement the estimation of fracture facies at different incidence and azimuthal angles. Comparisons between the estimated fracture facies and the reference fracture facies are shown in Figure 6. We observe there is a good match between the estimated and reference fracture facies.

We use the inversion results of EI of different incidence and azimuthal angles to obtain elastic properties (M and μ), density (ρ) and fracture weaknesses and employ the estimated fracture facies as the constraint. In Figure 7, we show comparisons between inversion

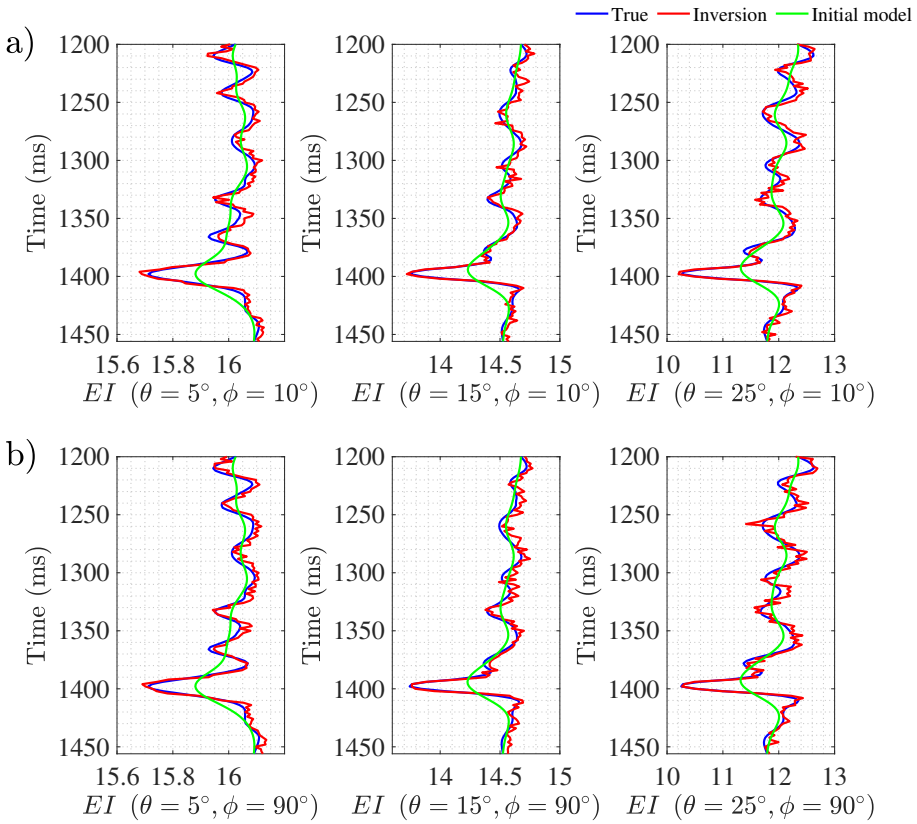

FIG. 4. Comparisons between true values and inversion results of EI of different incidence and azimuthal angles for the case of S/N of 4. a) Azimuthal angle ϕ is $10°$; and b) Azimuthal angle ϕ is $90°$.

results and true values of δ_N and δ_T, and we observe there is a good match between the true value and the inversion result obtained under the constraint of fracture facies.

CONCLUSION

We propose a two-step inversion method of employing azimuthally incidence-angle-stacked seismic data to estimate elastic parameters of isotropic background and the normal and tangential fracture weaknesses, in which fracture facies estimated during the estimation of azimuthal elastic impedance (EI) is employed as a constraint to improve the accuracy of inversion for fracture weaknesses. Using azimuthally incidence-angle-stacked seismic data as the input, we implement a Bayesian Markov chain Monte Carlo (MCMC) inversion for EI of different incidence and azimuthal angles, and predict fracture facies during the estimation of EI. Using the estimated EI as the input and the fracture facies as the constraint, we implement the estimation of elastic parameters and fracture weaknesses following a Bayesian framework again. We applying the proposed inversion method to noisy synthetic seismic data of different signal-to-noise ratios (S/N), and we observe that even in the case of S/N of 1, elastic parameters and fracture weaknesses are estimated stably. We conclude that the inversion method for estimating elastic parameters and fracture weaknesses constrained by fracture facies is robust.

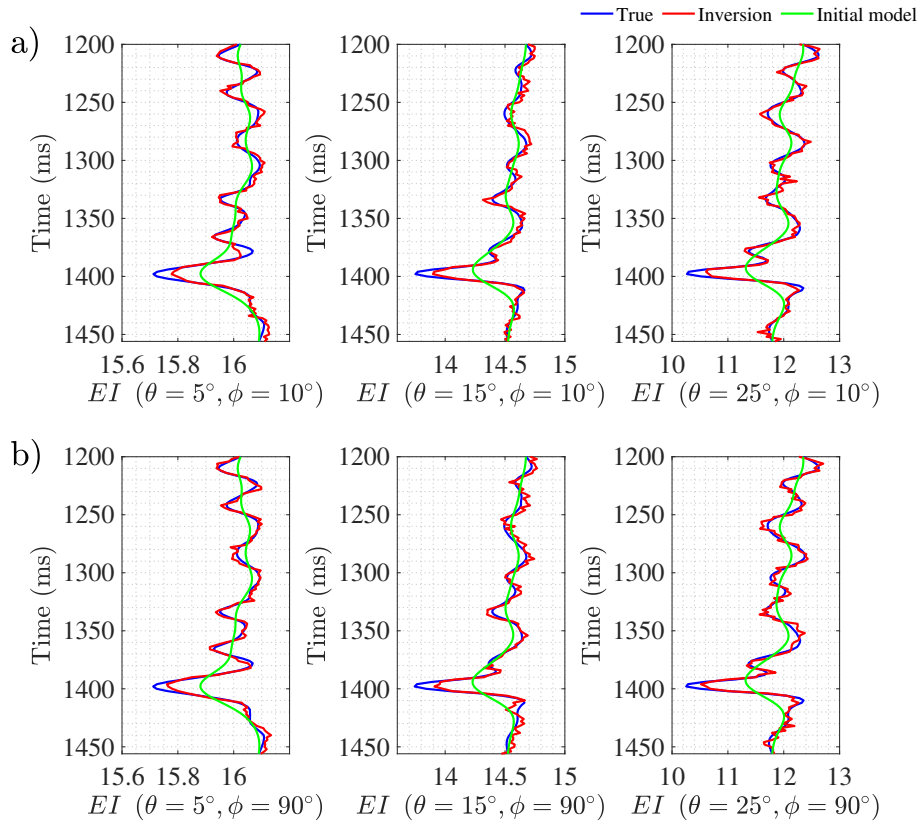

FIG. 5. Comparisons between true values and inversion results of EI of different incidence and azimuthal angles for the case of S/N of 1. a) Azimuthal angle ϕ is $10°$; and b) Azimuthal angle ϕ is $90°$.

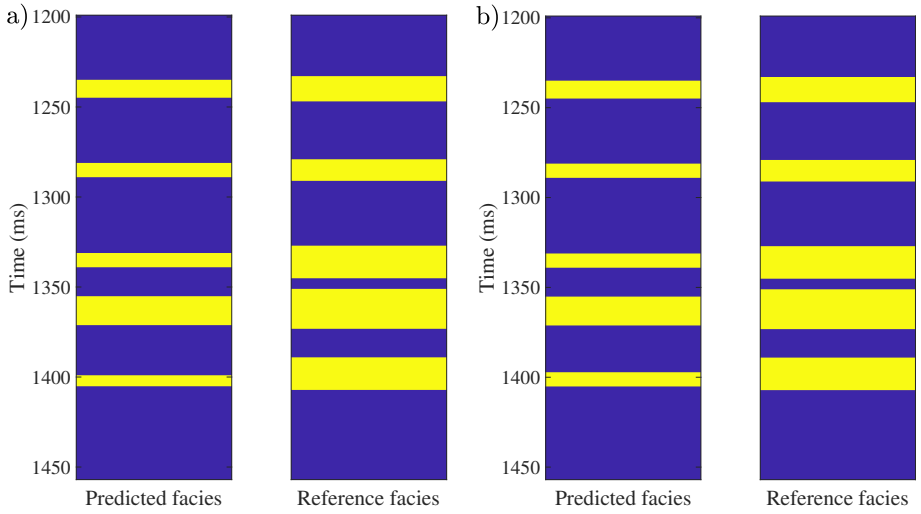

FIG. 6. Comparisons between the estimated fracture facies and the reference fracture facies. a) S/N of 4; and b) S/N of 1.

ACKNOWLEDGMENTS

We thank the sponsors of CREWES for continued support. This work was funded by CREWES industrial sponsors, and NSERC (Natural Science and Engineering Research Council of Canada) through the grant CRDPJ 461179-13.

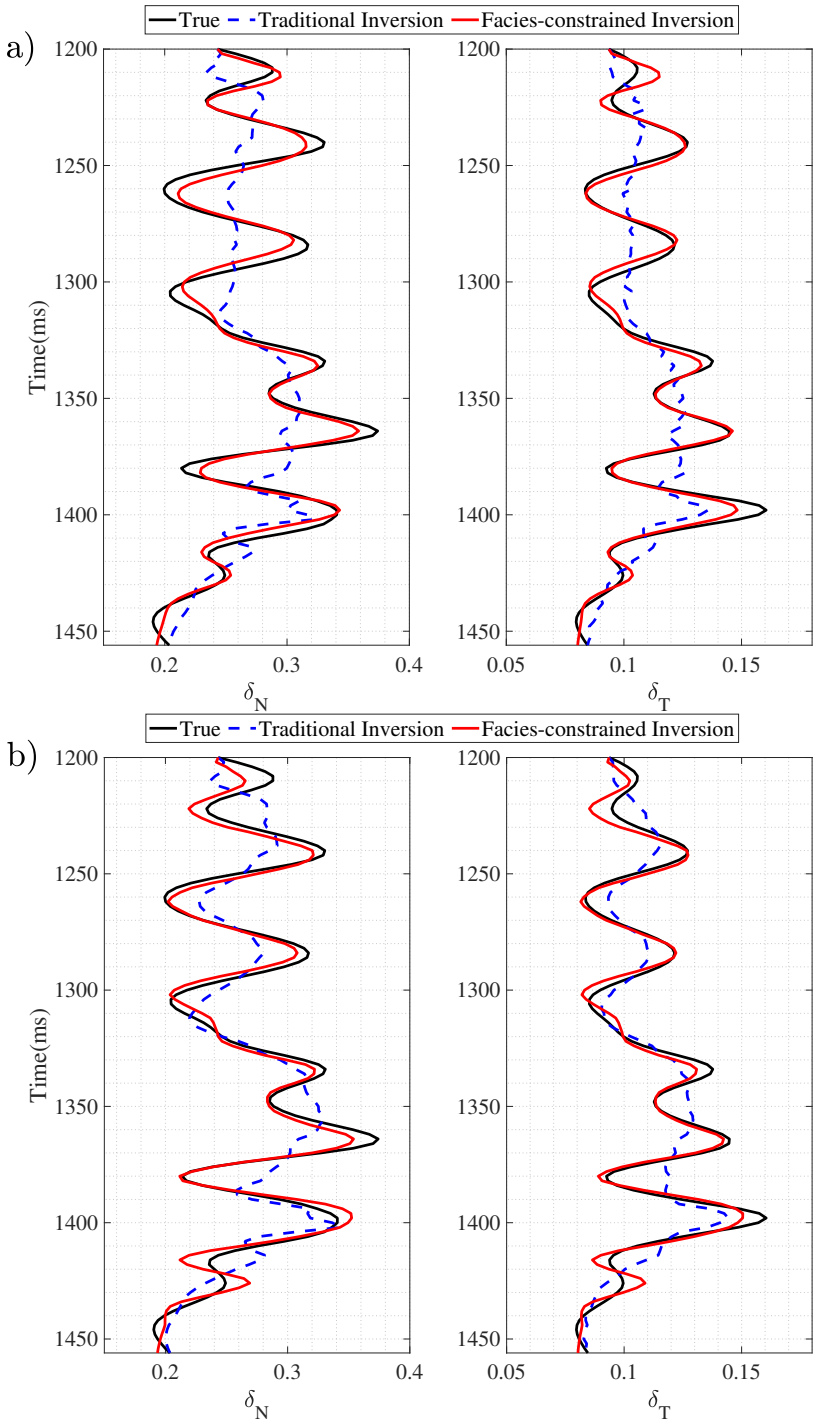

FIG. 7. Comparisons between true values and inversion results of fracture weaknesses. a) S/N of 4; and b) S/N of 1.

REFERENCES

Chen, H., Ji, Y., and Innanen, K. A., 2018, Estimation of modified fluid factor and dry fracture weaknesses using azimuthal elastic impedance: Geophysics, **83**, No. 1, WA73–WA88.

Chen, H., Zhang, G., Chen, J., and Yin, X., 2014, Fracture filling fluids identification using azimuthally elastic impedance based on rock physics: Journal of Applied Geophysics, **110**, 98–105.

Grana, D., 2018, Joint facies and reservoir properties inversion: Geophysics, **83**, No. 3, M15–M24.

Schoenberg, M., and Sayers, C. M., 1995, Seismic anisotropy of fractured rock: Geophysics, **60**, No. 1, 204–211.